Electronic Supplementary Material (ESI) for Physical Chemistry Chemical Physics.

Supporting information

On the relationship between Debye process in dielectric response and dissociation-association phenomenon in phenyl alcohols.

Anna Czaderna-Lekka[1]*, Magdalena Tarnacka[1]*, Zaneta Wojnarowska[1],
Barbara Hachuła[2], Marian Paluch[1], and Kamil Kamiński[1]

[1] *August Chełkowski Institute of Physics, University of Silesia in Katowice, 75 Pułku Piechoty 1, 41-500 Chorzów, Poland*
[2] *Institute of Chemistry, University of Silesia in Katowice, Szkolna 9, 40-006 Katowice, Poland.*

*Corresponding authors: (A.C.-L.) czanjo@gmail.com; (M.T.) magdalena.tarnacka@us.edu.pl.

Table of content

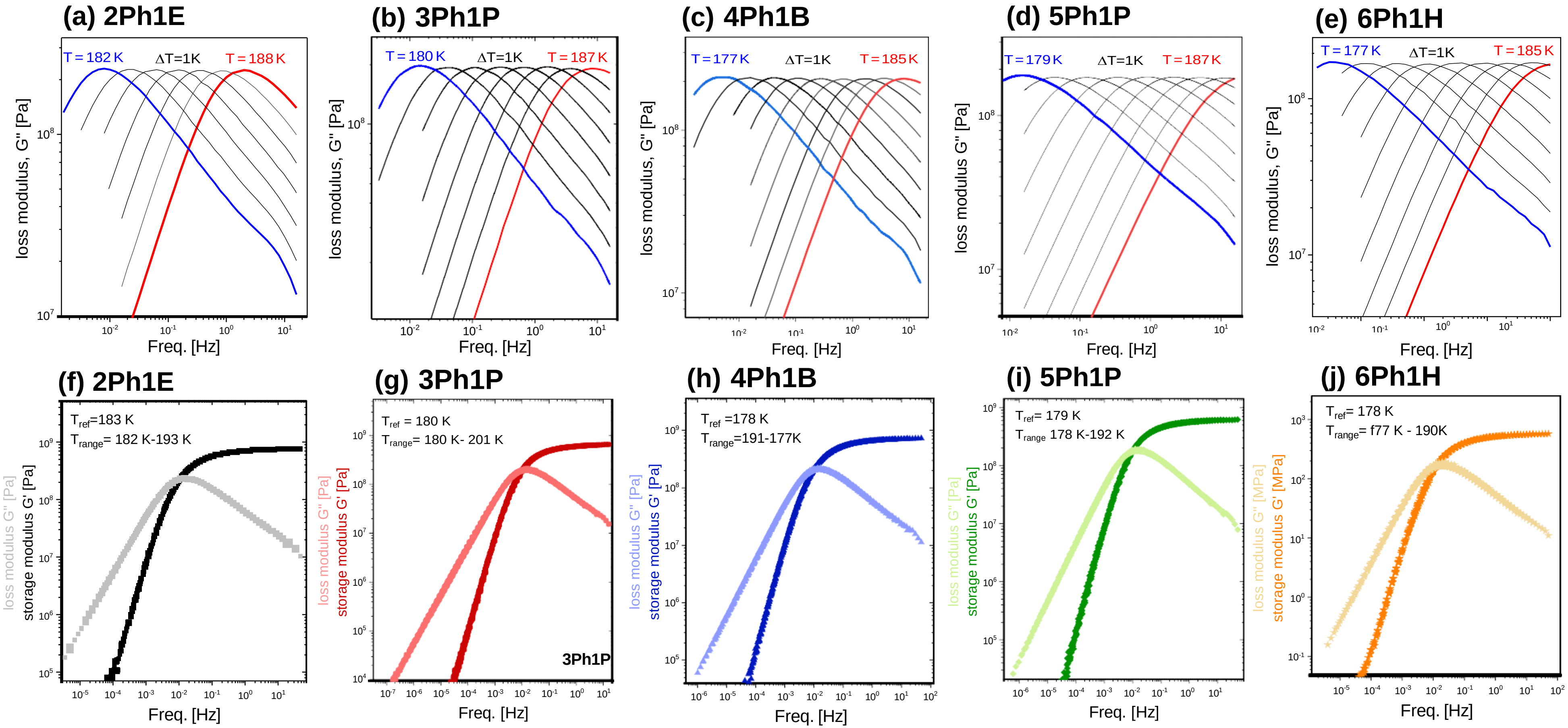

Figure S1. The frequency dependencies of loss modulus, *G''*, measured for all examined PhAs together with the master curves of measured storage, *G'*, and loss, *G''*, modulus.

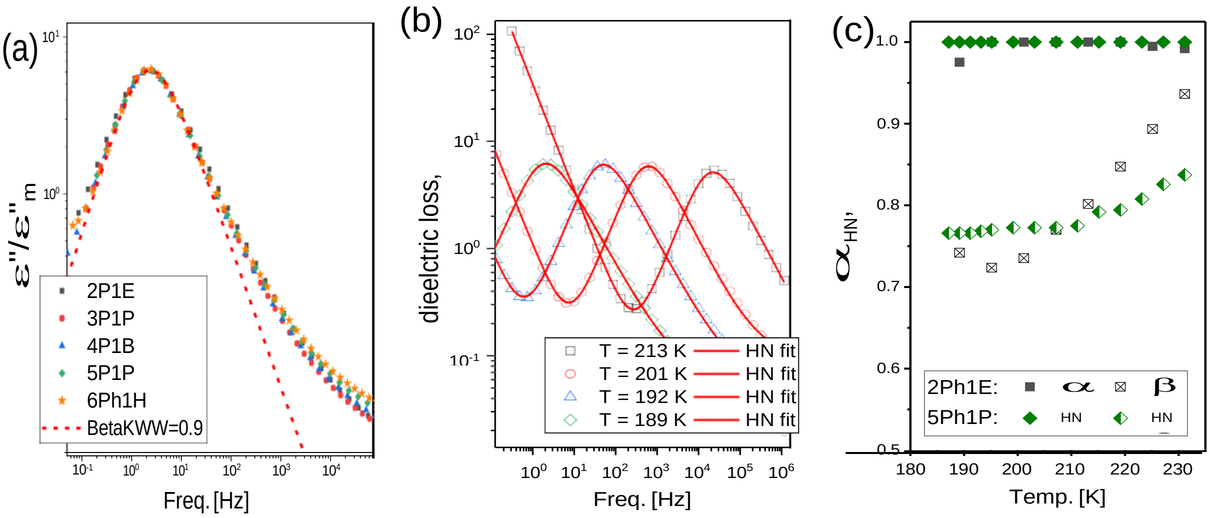

Figure S2. (a) The comparison of dielectric loss spectra of chosen PhAs at constant τD; (b) Dielectric spectra collected for 2Ph1E at indicated temperatures with the best fit to a single HN function with the conductivity term. Note that although the Debye process was only fitted with a single HN function, an additional contribution was included to the fitting due to the presence of secondary relaxation emerging at the high-frequency range. (c) Temperature dependences of HN shape parameters (αHN, βHN) of relaxation peaks obtained from HN fit of 2Ph1E and 5Ph1P.

Table S1. The VFT fitting parameters and the activation barrier of dissociation, $|E_{a,RM}|$, obtained from the RM for all examined PhAs analyzing data shown in **Figure 3**.

sample	$\log \tau_0$ [s]	D	T_0 [K]	$\lvert E_{a,RM}\rvert$ [kJ/mol]	$E_{a,vH}\rvert$[kJ/mol]
2Ph1E	-14.5	1196.3	149.7	14.2 ± 0.9	9.1 ± 0.3
3Ph1P	-12.4	815.6	154.6	14.3 ± 2.8	10.5 ± 0.3
4Ph1B	-12.6	972.9	150.7	13.2 ± 1.0	11.6 ± 0.2
5Ph1P	-12.4	727.2	155.0	13.3 ± 1.6	13.4 ± 0.8
6Ph1H	-12.9	872.0	150.4	12.9 ± 1.7	13.6 ± 0.4

It should be mentioned that for the majority of glass formers, dielectric spectra are usually shown in permittivity, ε^*, representation (**Figure 2(b)**). However, to compare results obtained by the two different experimental techniques, mechanical and dielectric, for a given material, it is often advised to use the same representation. Therefore, mechanical and dielectric data are presented in $G^*(\omega)$ and $M^*(\omega)$ representation, respectively. As one can recall, electric modulus and complex permittivity are related as follows:

$$M^*(\omega) = \frac{1}{\varepsilon^*(\omega)} = M'(\omega) + iM''(\omega) \qquad \text{(S1)}$$

where real (*M*’) and imaginary (*M*’’) parts of *M** have the following forms:

$$M'(\omega)=\frac{\varepsilon'(\omega)}{(\varepsilon'(\omega))^2+(\varepsilon''(\omega))^2} \quad \text{and} \quad M''(\omega)=\frac{\varepsilon''(\omega)}{(\varepsilon'(\omega))^2+(\varepsilon''(\omega))^2} \qquad \text{(S2)}$$

Using Eq. (S2), dielectric data were recalculated from *ε*”(ω) to *M*”(ω) as shown in **Figure S4**. Note that dielectric τ were calculated from the frequency of *M*” peak maximum ($\tau = 1/(2\pi f_{max})$).

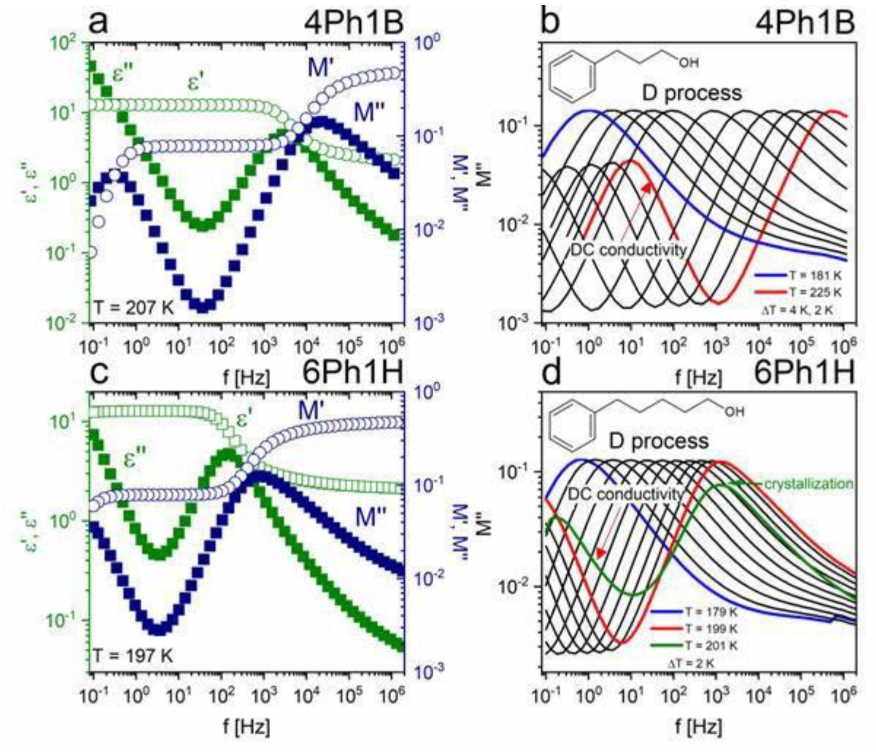

Figure S3. (a,c) Dielectric spectrum recorded for 4Ph1B (a) and 6Ph1H (c) at chosen temperature shown in electric modulus and dielectric permittivity representation. (b,d) The imaginary part of the electric modulus spectra used in further analysis of 4Ph1B (b) and 6Ph1H (d). The insets show the chemical structure of chosen PhAs.

Table S2. The activation barrier of dissociation, $|E_{a,RM}|$, for PhAs obtained for the analysis performed on relaxation times determined from the electric modulus, *M”*, representation.

sample	$\|E_{a,RM}\|$ [kJ/mol]
2Ph1E	19.4 ± 1.9
3Ph1P	20.2 ± 1.7
4Ph1B	20.4 ± 1.3
5Ph1P	12.2 ± 1.2
6Ph1H	13.0 ± 1.5

The van’t Hoff analysis

The MagicPlot software (version 2.9.3, MagicPlot Systems LLC, Saint Petersburg, Russia) was used to perform the O-H stretching bands' deconvolution process. The decomposition of this band into separate components involved the three steps as follows (i) the curve fitting of the band occurring between 3050 and 3800 cm^{-1} carried out with the use of two Gaussian functions adjusting the intensity and the width of the curves, (ii) the subtracting the fitted spectrum of H-bonded band from the original I.R. spectra, (iii) the peak fitting of the free O-H band occurring between 3600 and 3650 cm^{-1}. It was important to accurately determine the H-bonded O-H band's spectral parameters since it strongly affected the free O-H band's final intensities and bandwidths. Both free and H-bonded OH band components were not involved in the decomposition together because a large error is obtained during the fitting of a poorly resolved broad OH band with multiple components. In addition, we used the described deconvolution procedure to remove the contribution of H-bonded OH groups from the free hydroxyl groups. In this way, we obtained a better fitting of the peak of free OH groups occurring above the 3600 cm^{-1} frequency range.

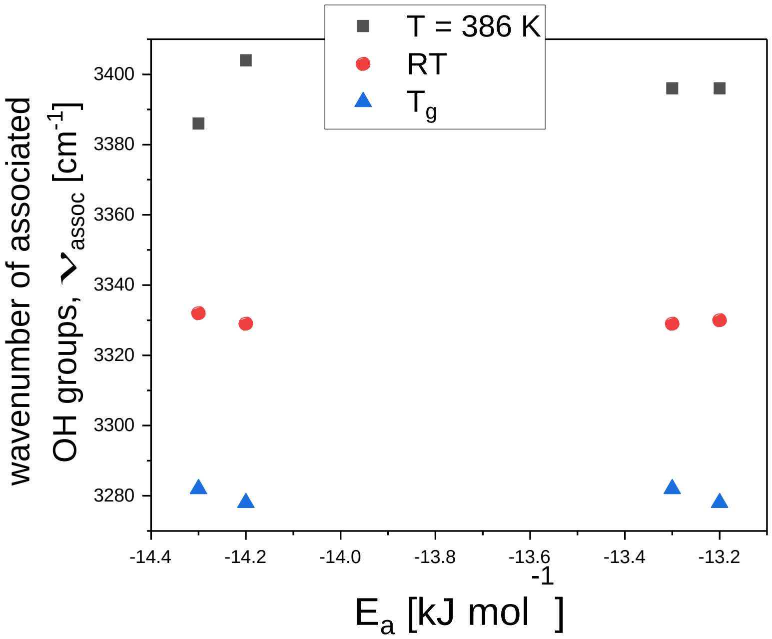

Figure S4. The wavenumber of broad band related to values of stretching vibration of associated (H-bonded) OH groups, ν_{assooc}, plotted versus the activation energy, E_a, extracted from the Rubenstein model (Eq. 1).